Influence of Packing on Low Energy Vibrations of Densified Glasses

Giovanni Carini, Jr.,[1] Giuseppe Carini,[2] Giovanna D'Angelo,[2] Gaspare Tripodo,[2] Gaetano Di Marco,[1] Cirino Vasi,[1] and Edmondo Gilioli[3]

[1]*IPCF del C.N.R., Sede di Messina, I-98158 Messina, Italy*

[2]*Dipartimento di Fisica e di Scienze della Terra, Università degli Studi di Messina, I-98166 Messina, Italy*

[3]*IMEM del C.N.R., Area delle Scienze, I-43010 Parma, Italy*

(Received 22 July 2013; published 11 December 2013)

A comparative study of Raman scattering and low temperature specific heat capacity has been performed on samples of B_2O_3, which have been high-pressure quenched to go through different glassy phases having growing density to the crystalline state. It has revealed that the excess volume characterizing the glassy networks favors the formation of specific glassy structural units, the boroxol rings, which produce the boson peak, a broad band of low energy vibrational states. The decrease of boroxol rings with increasing pressure of synthesis is associated with the progressive depression of the excess low energy vibrations until their full disappearance in the crystalline phase, where the rings are missing. These observations prove that the additional soft vibrations in glasses arise from specific units whose formation is made possible by the poor atomic packing of the network.

DOI: 10.1103/PhysRevLett.111.245502 PACS numbers: 63.50.Lm, 65.60.+a, 78.30.Ly

Glasses exhibit an excess of low energy vibrational modes over the classical Debye density of states whose nature is far from an exhaustive understanding. These collective modes range between 0.1 and 3 THz and contribute to (i) the boson peak (BP) in inelastic light (Raman) and neutron scattering spectra, (ii) the excess low temperature (1–20 K) heat capacity C having the shape of a broad hump when reported as C_p/T^3, and (iii) the plateau of the thermal conductivity $k(T)$ at around 10 K [1–3]. All these experimental findings exhibit a remarkable universality and are usually ascribed to an excess of low energy excitations, which exist beside phonons and take their origin from the disordered topology of amorphous structures. Glass densification offers the possibility to learn more about the nature of low energy vibrations because it leads to significant modifications of the short- and medium-range orders and to a reduction of the atomic mobility without altering the stoichiometry [4–6]. To follow the correlation between low energy vibrational modes and the structural changes implying only modification of the medium-range order, we have performed Raman scattering and low temperature heat capacity experiments on compacted samples of B_2O_3. These solids have been high-pressure quenched to go through different glassy phases having growing density to the crystalline state. Increasing density leads to the decrease of boroxol rings, the superstructural units formed by three corner sharing BO_3 triangles in vitreous B_2O_3 (v-B_2O_3) [7], and to the progressive depression of the BP and the excess specific heat capacity between 1.5 and 30 K until their full disappearance in the crystalline phase.

Sample densification was obtained by loading $^{11}B_2O_3$ glasses in a multianvil high temperature and pressure apparatus for the synthesis at 2 and 4 GPa [5]. They were fused under pressure at 1160 °C (2-GPa glass) and at 1060 °C (4-GPa/$B3$ glass) for about 20 min and then quenched at those pressures. Densified B_2O_3 glasses were characterized by x-ray diffraction which revealed no sign of crystallization. Crystalline samples (c-B_2O_3) were obtained by fusing $^{11}B_2O_3$ glasses at 1280 °C under a pressure of 4 GPa for about 15 min and then pressure quenched to room temperature. The x-ray diffraction pattern of polycrystalline samples gave well-defined peaks, typical of trigonal crystalline B_2O_3 (α-B_2O_3) [8]. The densities measured at room temperature are 1826 kg/m^3 (v-B_2O_3), 2082 kg/m^3 (2-GPa glass), and 2174 kg/m^3 (4-GPa/$B3$ glass). The density of c-B_2O_3 is 2560 kg/m^3 [8]. The Debye sound velocity v_D ($\frac{3}{v_D^3} = (1/v_l^3) + (2/v_t^3)$) and the elastic Debye temperature Θ_D have been determined by the values of longitudinal (v_l) and shear (v_t) sound velocities measured at 8 K [6]: $v_D = 2095$ m/s, $\Theta_D = 260.3$ K (v-B_2O_3); $v_D = 2436$ m/s, $\Theta_D = 317.7$ K (2-GPa glass); and $v_D = 3417$ m/s, $\Theta_D = 454.9$ K (4-GPa/$B3$ glass). The Raman spectra were performed at room temperature on a double monochromator Jobin-Yvon U-1000 and were recorded in 90° scattering geometry using the same procedure described elsewhere [5]. The specific heat capacity of B_2O_3 samples was measured using an automated calorimeter, which operated via the thermal relaxation method in a ^{4}He cryostat [2]. The Raman spectra of normal and densified v-B_2O_3 between 6 and 1000 cm^{-1} are shown in Fig. 1(a) for a VV (polarized) configuration. The spectra have been normalized by the total integrated intensity of the multicomponent band between 1200 and 1600 cm^{-1} [see Fig. 1(b)] which reflects the vibrations of all the units forming the whole glassy network [5]. Densification gives rise to a parallel and progressive decrease of both the BP and the highly

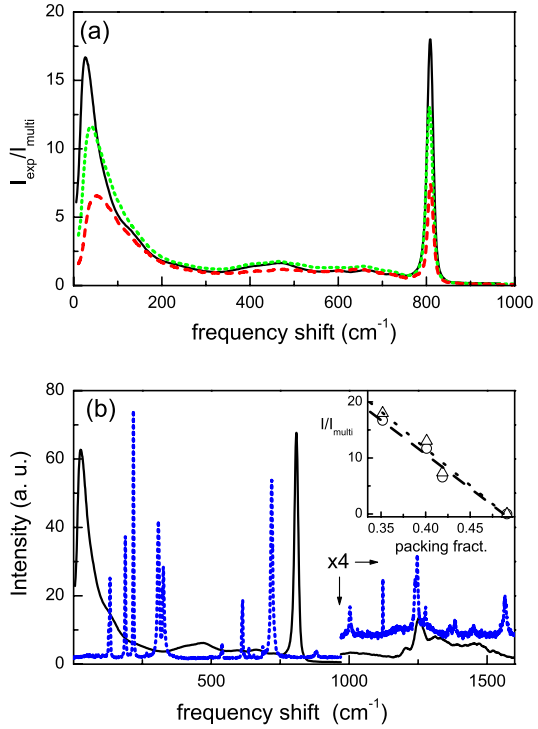

FIG. 1 (color online). (a) Raman intensity I_{exp} normalized by the integrated intensity of the high-frequency multiband I_{multi} of densified B_2O_3 glasses for VV polarization: v-B_2O_3, solid line; 2-GPa glass, dotted line; and 4-GPa/$B3$ glass, dashed line. (b) Raman spectra of v-B_2O_3 (solid line) and c-B_2O_3 (dotted line). Above 970 cm^{-1}, the y scale is expanded by 4. The inset shows the behaviors of the normalized intensities of the BP (circles) and of the band at 808 cm^{-1} (triangles) vs the atomic packing fraction Φ.

polarized band at 808 cm^{-1}, the latter arising from a localized breathing-type vibration of oxygen atoms inside the plane boroxol ring. Differently from the band at 808 cm^{-1}, which strictly preserves its frequency with densification, the frequency ν_{BP} of BP increases from 26 cm^{-1} in normal B_2O_3 to about 52 cm^{-1} in 4-GPa/$B3$ glass. The low-frequency Raman intensity is related to number of vibrational excitations, given by the product between the vibrational density of states $g(\nu)$ and the Bose factor for the Stokes component $[n(\nu) + 1]$, via the ratio between the light-vibration coupling coefficient $C(\nu)$ and ν [9]: $I(\nu) = C(\nu)g(\nu)[n(\nu) + 1]/\nu$. Over the frequency region of BP, $C(\nu)$ exhibits a nearly linear frequency dependence [10], implying a direct proportionality between the Raman intensity and the number of vibrational excitations.

Raman spectra of v-B_2O_3 and c-B_2O_3 are compared in Fig. 1(b), showing the disappearance of the band at 808 cm^{-1} in the crystal. The lines observed in c-B_2O_3 strictly correspond to those revealed in a previous study by Bronswjik and Struijks [11] and prove that its structure is built on infinite chains of BO_3 triangles [8] and does not contain boroxol rings. As recently emphasized by nuclear magnetic resonance [4] and Raman scattering [5] studies and confirmed by the present results, melt quenching under pressure up to 4 GPa of B_2O_3 prevents the transformation of BO_3 chainlike segments in rings during the cooling process. Increasing densification by pressure leads the system towards a structure having a progressively decreasing content of rings until their full disappearance in the crystal characterized by the most efficient packing of BO_3 units. It is worth noting that the decrease of rings is paralleled by a strikingly similar reduction of the BP which, as expected, is missing in c-B_2O_3. The first feature observed in the crystal is the optical mode at 132 cm^{-1}, also visible as a shoulder on the high-frequency tail of the BP in the glass. The inset of Fig. 1(b) reports the normalized intensities of the BP and the band at 808 cm^{-1} vs the atomic packing fraction Φ [12,13], which changes from 0.35 in v-B_2O_3 to 0.49 in c-B_2O_3. Both the bands show a very close linear decrease with increasing Φ, pointing to zero in correspondence to the value of the crystal.

This observation indicates a strong correlation between the boroxol ring population and the vibrations underlying the BP, disclosing that these excess modes must be associated with low energy vibrations of these glassy structural units. The specific heat capacities $C_p(T)$ of densified B_2O_3 glasses are compared with that of c-B_2O_3 in Fig. 2(a). The present data are in very close agreement with earlier experimental observations in v-B_2O_3 above 2 K [14] and in c-B_2O_3 above 18 K [15], also included in the same figure. In the case of crystalline dielectrics, phonons dominate the thermal properties: $C_p(T)$ of c-B_2O_3 follows strictly the Debye T^3 law [dotted line in Fig. 2(a)] giving a Debye temperature $\Theta_D = 621$ K. All the glasses show an excess $C_p(T)$ over the heat capacity of the crystalline sample. When plotted as $C_p(T)/T^3$ vs T [Fig. 2(b)], it results in the characteristic shape of a broad peak with a magnitude substantially larger than the respective elastic Debye contributions $C_D(T)$. Growing densification depresses $C_p(T)$ over the whole temperature interval explored, giving rise to a significant decrease of the bump and to an increase of the peak temperature T_{peak}, which shifts from about 5.7 K in v-B_2O_3 to about 10.0 K in 4-GPa/$B3$ glass. To compare the changes of the excess specific heat with the modifications of the elastic continuum, we report $C_p(T)$ scaled by $C_D(T)$ of densified B_2O_3 glasses vs T/Θ_D in the inset of Fig. 3(a). $C_p(T)/C_D$ increases with increasing densification, also exhibiting a well-defined shift of the maxima. This finding implies a variation of T_{peak} stronger than that experienced by Θ_D and changes of the low energy vibrational dynamics which are not accounted for by the transformations of the elastic continuum. Scaling the bumps observed in all the glasses by $(C_p/T^3)_{peak}$, we obtain curves showing an identical shape [Fig. 3(a)]. This observation reflects the invariance of the shape of the scaled BP revealed by Raman scattering [5] and confirms the results of similar studies in compacted glasses of SiO_2 [16] and GeO_2 [17]. This invariance discloses a low energy

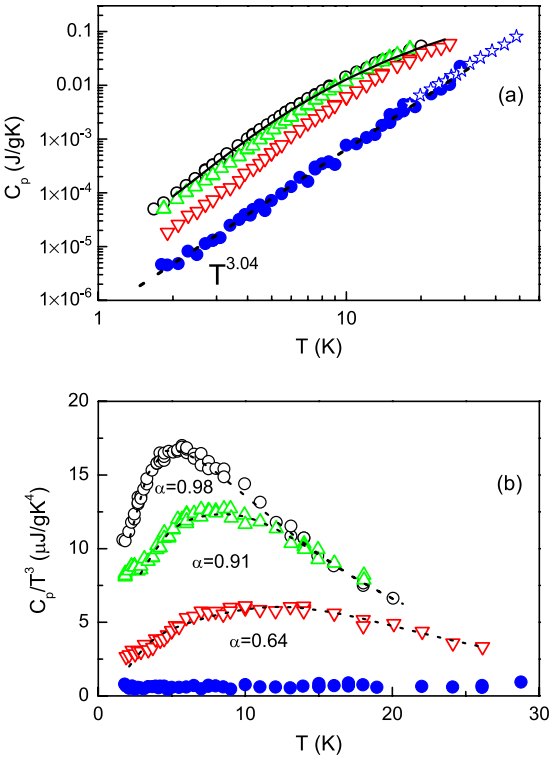

FIG. 2 (color online). (a) The temperature dependence of the specific heat capacity C_p in B_2O_3 samples: v-B_2O_3 (empty circles), 2-GPa glass (up triangles), 4-GPa/$B3$ glass (down triangles), and c-B_2O_3 (full circles). Earlier experimental observations on v-B_2O_3 [14] and c-B_2O_3 [15] are reported for comparison as a solid line and stars, respectively. The dotted line represents a fit to the data between 2 and 8 K of c-B_2O_3, which gives a $T^{3.04}$ behavior. (b) $C_p(T)/T^3$ for densified B_2O_3 glasses and c-B_2O_3; the symbols are those of (a). Dotted lines represent the fit by Eq. (1) to the data using $g(\nu)$ evaluated from the Raman spectra with $C(\nu) \sim \nu^{\alpha}$.

vibrational dynamics underlying the BP where all the modes, extended and localized, are coupled and hybridized, resulting in an overall spectral distribution which is independent of the packing fraction of the system. We can evaluate the density of low energy vibrational states (DVS) and its behavior with increasing density in compacted glasses by using $g(\nu)$ derived by the low-frequency Raman intensity to determine the temperature dependence of the low temperature heat capacity expressed by the usual equation:

$$C_p \approx C_V = 3Nk_B \int_0^{\nu_o} g(\nu)\left(\frac{h\nu}{k_BT}\right)^2 \times \frac{\exp(h\nu/k_BT)}{[\exp(h\nu/k_BT)-1]^2} d\nu, \quad (1)$$

where N is the number density and ν_o the highest vibrational frequency. The main problem in determining $g(\nu)$ from the normalized Raman intensity is that it gives the product between $g(\nu)$ and $C(\nu)$. In v-B_2O_3, however, it has been shown that $C(\nu)$ follows a linear frequency dependence over the frequency range between 9 cm^{-1} ($0.5\nu_{BP}$) and 36 cm^{-1} ($2\nu_{BP}$), deviating from this behavior at lower (superlinear) and higher (sublinear) frequencies [10,18]. We assume $C(\nu) \sim \nu^{\alpha}$ to account for possible variations of the exponent α with densification and also use the magnitude of $g(\nu)$ as a further fitting parameter [19]. A further problem arises from the quasielastic scattering (QS) due to a fast relaxation, which exhibits a temperature dependence much larger than the Bose factor and dominates the frequency region below about 20 cm^{-1} [20]. It is usual to perform low temperature (below 100 K) measurements of inelastic neutron and Raman scattering in order to depress all the relaxation mechanisms which are the source for QS [18,19]. However, light scattering measurements of fast relaxation in v-B_2O_3 between 15 and 300 K showed that QS affects significantly the low-frequency spectra only up to about 10–12 cm^{-1} [21]. Moreover, growing densification is expected to depress the relaxation mechanism giving rise to QS [6]. This evidence leads us to use the present room temperature Raman spectra for evaluating the spectral dependence of $g(\nu)$ down to about 12 cm^{-1}, approximating its behavior to lower frequencies by the Debye density of states $g_D = 3(\nu^2/\nu_D^3)$ determined by the values of $\nu_D = k_B\Theta_D/h$. We also consider the Raman intensity up to 90 cm^{-1}, in order to avoid contributions from optical modes [Fig. 1(b)], which can have a coupling coefficient quite different from the vibrations causing the BP. The experimental results of $C_p(T)/T^3$ are compared to the theoretical fit in Fig. 2(b), where the resulting values for the exponent α are also included. It is worth noting that small variations of α (less than 5%) lead to unacceptable fitting curves. The decrease of α with increasing packing fraction is surely due to significant modifications of the static fluctuations of elasto-optical constants, which are the expected sources for $C(\nu)$ behavior [20]. The obtained DVSs, plotted as $g(\nu)/\nu^2$ in Fig. 3(b), show the BP above the respective elastic Debye levels for all the glasses, at least up to about 1.5 THz. Increasing packing fraction shifts the BP from 18 cm^{-1} in v-B_2O_3 up to 35 cm^{-1} in 4-GPa/$B3$ glass, progressively depressing the excess vibrational modes. Despite the rough evaluation of $g(\nu)$ due to approximations used, there is a reasonable agreement between the present result in v-B_2O_3 and the DVS determined by inelastic neutron scattering at 100 K [18] with a close coincidence of the BP frequency. The present observations prove unambiguously that the systematic density increase of v-B_2O_3, associated with the progressive decrease of boroxol rings, causes the reduction of both the BP and the excess heat capacity until their disappearance in the crystal, whose low energy vibrational dynamics is fully described by the Debye model [Fig. 2(a)].

We remark that, in addition to boroxol rings, some further superstructural units can characterize the network

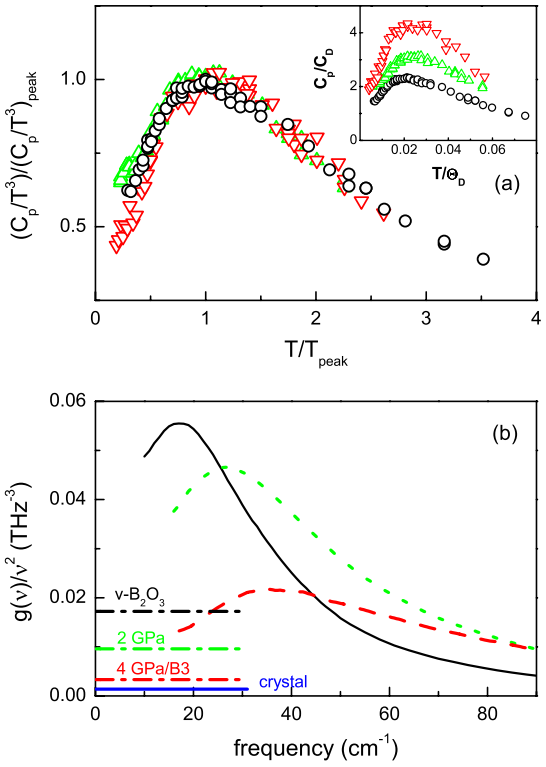

FIG. 3 (color online). (a) Comparison of the specific heats of densified B_2O_3 glasses, plotted as $C_p(T)/T^3$ scaled by $(C_p/T^3)_{\text{peak}}$ vs T/T_{peak}: v-B_2O_3 (empty circles), 2-GPa glass (up triangles), and 4-GPa/$B3$ glass (down triangles). The inset shows $C_p(T)/C_D$ vs T/Θ_D. (b) Reduced density of low energy vibrational modes $g(\nu)/\nu^2$ in densified B_2O_3 glasses as deduced from the fits to specific heat capacity data: v-B_2O_3, solid line; 2-GPa glass, dotted line; and 4-GPa/$B3$ glass, dashed line. The Debye levels are reported as dash-dotted lines for glasses and a solid line for c-B_2O_3.

of compacted glasses and cause an excess vibrational contribution. We can exclude the formation of superstructural units containing BO_4 groups which should cause a band at 775 cm^{-1} [5], not observed in the present Raman spectra; thus, the above units could arise from the breaking up of rings in the melt under pressure which originates the formation of larger puckered rings made up of connected BO_3 triangles and folded on themselves [7]. They are surely preserved in pressure-quenched glasses also contributing to the observed increase of the packing. It is expected that these large rings can also be a source for additional localized low energy vibrations contributing to both the BP and the excess heat capacity.

This evidence leads us to assign the large excess $C_p(T)$ and the vibrational dynamics underlying the BP to low energy modes mainly arising from boroxol rings. Following the findings of a refined study of hyper-Raman and Raman scattering in v-B_2O_3 by Simon *et al.* [22], we assign these modes to out-of-plane rigid librations of planar boroxol rings. The rings are formed due to the poor atomic packing of the glassy network and can be connected either via a single oxygen atom bridging two rings or via one or several planar BO_3 triangles [23]. The latter need a larger volume than the former, and their formation is expected to be more prevented with increasing densification. The observed network hardening and frequency increase of the BP with densification should be related to the gradual disappearance of rings connected by more complex links than a single bridging oxygen. The existence of specific structural units making up the glassy network and producing an excess of low energy vibrations is not limited to v-B_2O_3, but it has been found in other prototype glasses. In v-SiO_2, the DVS obtained by inelastic neutron scattering has been satisfactorily modeled by considering coupled rotations of connected SiO_4 tetrahedra [24], this finding having been confirmed by a more recent study of hyper-Raman scattering [25]. In v-Se, a low energy DVS, which accounts at most qualitatively for the low temperature anomalies in the thermal properties, was determined by molecular dynamics simulation assuming torsional librations of Se chains [26].

Moreover, in v-Se, there are eight atom rings (Se_8) which do not exist in the trigonal crystalline form, an array of parallel chains arranged on a two-dimensional hexagonal lattice [27]. The Se_8 rings could be the source for additional soft vibrations. A polycrystalline sample of hexagonal Se, in fact, evidenced a Debye behavior for the specific heat capacity below 10 K with a magnitude substantially smaller than that of the corresponding glass [28]. To conclude, experiments have been presented in which the low temperature vibrational specific heat and the low-frequency Raman scattering have been directly compared, for the first time, within B_2O_3 solids with increasing density from the glassy to the crystalline phases. The results show that the formation of superstructural units, such as boroxol rings, in the glass gives rise to a broad spectrum of low-lying vibrations over the Debye-like acoustic waves. Since the excess heat capacity of B_2O_3 glasses can be reproduced using the BP observed in the Raman spectra, the physical nature of the large distribution of additional soft vibrations, which determine the low temperature thermal and low-frequency optical properties of a glass, has now been clarified.

[1] T. Nakayama, Rep. Prog. Phys. **65**, 1195 (2002).
[2] G. D'Angelo, G. Carini, C. Crupi, M. Koza, G. Tripodo, and C. Vasi, Phys. Rev. B **79**, 014206 (2009).
[3] G. D'Angelo, C. Crupi, G. Salvato, G. Tripodo, and C. Vasi, J. Phys. Chem. B **114**, 2467 (2010).
[4] V. V. Brazhkin, I. Farnan, K. I. Funakoshi, M. Kanzaki, Y. Katayama, A. G. Lyapin, and H. Saitoh, Phys. Rev. Lett. **105**, 115701 (2010).
[5] G. Carini, Jr., E. Gilioli, G. Tripodo, and C. Vasi, Phys. Rev. B **84**, 024207 (2011).

[6] G. Carini, Jr., G. Carini, G. Tripodo, G. Di Marco, and E. Gilioli, Phys. Rev. B **85**, 094201 (2012).
[7] A. C. Wright, G. Dalba, F. Rocca, and N. M. Vedischcheva, Phys. Chem. Glasses: Eur. J. Glass Sci. Technol. B **51**, 233 (2010).
[8] G. E. Gurr, P. W. Mongotmery, C. D. Knutson, and B. T. Gorres, Acta Crystallogr. Sect. B **26**, 906 (1970).
[9] R. Shuker and R. W. Gammon, Phys. Rev. Lett. **25**, 222 (1970).
[10] N. V. Surovtsev and A. P. Sokolov, Phys. Rev. B **66**, 054205 (2002).
[11] J. P. Bronswjik and E. Struijks, J. Non-Cryst. Solids **24**, 145 (1977).
[12] The packing fraction is defined as $\phi = N_A V_{\text{atomic}}/V_{\text{molar}}$, V_{molar} being the molar volume and V_{atomic} the ionic volume. The ionic radii are taken from Ref. [13], accounting for the typical coordination of the network forming ions.
[13] R. D. Shannon, Acta Crystallogr. Sect. A **32**, 751 (1976).
[14] G. K. White, S. J. Collocott, and J. S. Cook, Phys. Rev. B **29**, 4778 (1984).
[15] E. C. Kerr, H. N. Hersh, and H. L. Johnston, J. Am. Chem. Soc. **63**, 1137 (1941).
[16] X. Liu, H. v. Lohneysen, G. Weiss, and J. Arndt, Z. Phys. B **99**, 49 (1995).
[17] L. Orsingher, A. Fontana, G. Carini, Jr., G. Carini, G. Tripodo, T. Unruh, and U. Buchenau, J. Chem. Phys. **132**, 124508 (2010).
[18] D. Engberg, A. Wischnewski, U. Buchenau, L. Borjesson, A. J. Dianoux, A. P. Sokolov, and L. M. Torell, Phys. Rev. B **58**, 9087 (1998).
[19] A. Fontana, F. Rossi, G. Carini, G. D'Angelo, G. Tripodo, and A. Bartolotta, Phys. Rev. Lett. **78**, 1078 (1997).
[20] J. Jackle, in *Amorphous Solids: Low-Temperature Properties*, edited by W. A. Phillips (Springer, Berlin, 1981), p. 135.
[21] N. V. Surovtsev, J. A. H. Wiedersich, E. Duval, V. N. Novikov, E. Rossler, and A. P. Sokolov, J. Chem. Phys. **112**, 2319 (2000).
[22] G. Simon, B. Hehlen, E. Courtens, E. Longueteau, and R. Vacher, Phys. Rev. Lett. **96**, 105502 (2006).
[23] F. L. Galeener and M. F. Thorpe, Phys. Rev. B **28**, 5802 (1983).
[24] U. Buchenau, M. Prager, N. Nucker, A. J. Dianoux, N. Ahmad, and W. A. Phillips, Phys. Rev. B **34**, 5665 (1986).
[25] B. Hehlen, E. Courtens, R. Vacher, A. Yamanaka, M. Kataoka, and K. Inoue, Phys. Rev. Lett. **84**, 5355 (2000).
[26] F. J. Bermejo, E. Enciso, A. Criado, J. L. Martinez, and M. Garcia-Hernandez, Phys. Rev. B **49**, 8689 (1994).
[27] R. M. Martin, G. Lucovsky, and K. Helliwell, Phys. Rev. B **13**, 1383 (1976).
[28] A. Avogadro, S. Aldovrandi, F. Borsa, and G. Carini, Philos. Mag. B **56**, 227 (1987).